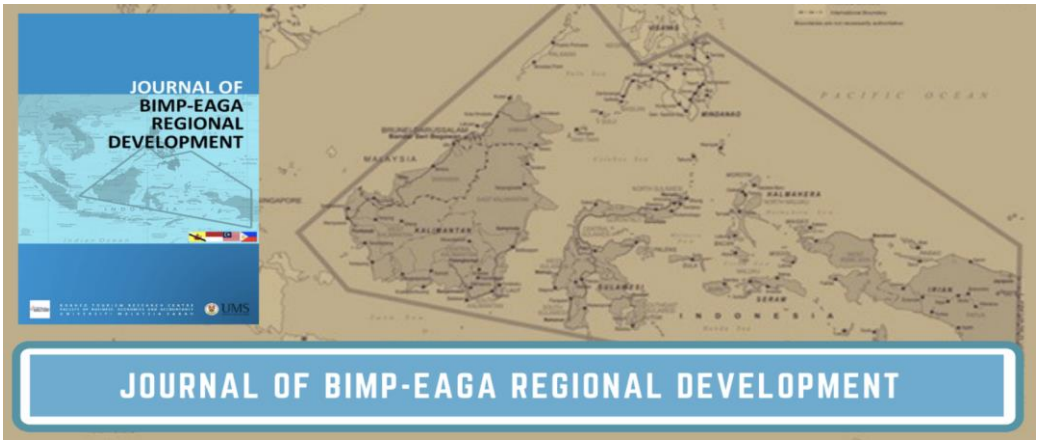

Improving the self-starting ability of small VAWT by improving the blade shape

Yuta Odanaga[a],Mizuyasu Koide[a]

[a]*National Institute of Technology,Fukushima College,30 Nagao,Kamiarakawa,Taira,Iwaki,Fukushima,970-8034,Japan*

Abstract

A vertical－axis wind turbine (VAWT) is a wind turbine that axis of rotation is perpendicular to the ground. This type of wind turbine is omnidirectional and is expected to have potential for use in urban and city areas with unstable wind conditions. However, they have the disadvantage of poor self-starting performance. Studies have been conducted to improve self-starting performance by using a wind collector plate and by devising the location of the wind turbine, but no decisive improvement has yet been achieved. In this research, wind tunnel tests and CFD were conducted on a small VAWT with an existing blade shape to clarify its power characteristics, and the possibility of using blade end plates and flaps was also investigated. In the low-velocity range, the drag-type wind turbine showed superior self-starting performance, but the torque decreased when the blade was in a certain attitude. In the experiment with the blade end plates, the torque was up to 155% of that without the plates. The flaps on a lift-type wind turbine reduce the flow velocity on the underside of the blade, resulting in higher values of both lift and drag. Therefore, it can be considered that the installation of flaps contributes to improving the self-starting performance of lift-type wind turbines.

Keywords: CFD, Self-starting, Vertical Axis Wind Turbine (VAWT), Wind Turbine

1. Introduction

Rapid global warming has been progressing in recent years. The global average temperature has increased by 0.76°C in 100 years [(1)]. The main cause of global warming is the increase in greenhouse gases emitted from the use of fossil fuels.

Thermal power generation accounts for about 70% of power generation in Japan. Whereas, the use of renewable energy sources, which do not emit greenhouse gases, is only about 12%. In the world, the percentage of electricity generated from renewable energy sources in other countries is 43.6% in Germany and 43.1% in the U.K[(2)]. Wind

Corresponding author: Mizuyasu Koide
Received: 2.03.2025
Accepted: 5.03.2025
Revised: 14.03.2025
Published: 17.03.2025
DOI: 10.51200/jberd.v11i1.6224

power, the subject of this study, is a type of renewable energy, and its introduction is increasing year by year. Figure 1 shows the installed capacity of wind power generation in Japan from 2010 to June 2022.

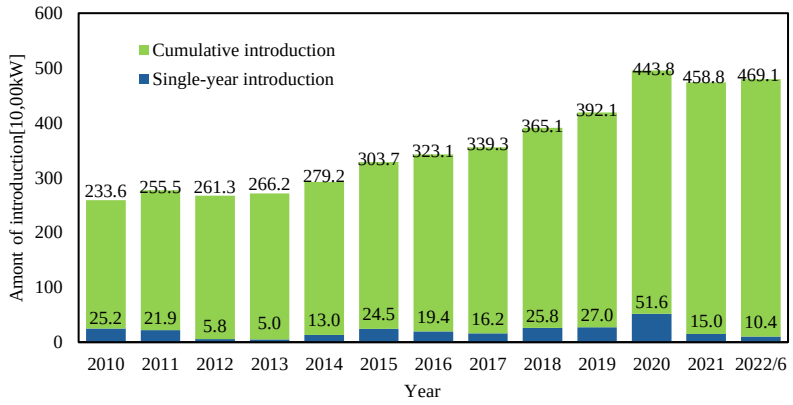

Fig. 1 Trends in Wind Power Generation in Japan [3]

At the end of 2022, the world's cumulative installed base of wind power was 906 GW, up 9% from the end of 2021. 77.6 GW of new wind power was installed in 2022. Of the new installations, 49% are in China, 11% in the United States, and 25% in Europe. Japan accounts for 0.5% of the world's total installed capacity of 4804 MW, and 0.3% of the world's new installed capacity of 233 MW. Japan is out of the top 16 in terms of installed capacity. China is aggressively introducing offshore wind power, with 68.6 MW in 2020 and 16.9 MW in 2021 [4]. In 2021, subsidies for the introduction of wind turbines were abolished, resulting in a smaller amount being introduced. However, by the end of 2022, China's installed renewable energy capacity will reach 1213 GW, surpassing coal-fired power generation for the first time.

Figure 2 shows the production capacity of blades, generators, and gearboxes for wind power generators. The global wind power industry is heavily dependent on China, and Japan's share of the global wind power industry is extremely small. Therefore, it is expected that the further diffusion of wind power generation in Japan and the increase in the number of wind power installations around the world will help reduce greenhouse gas emissions.

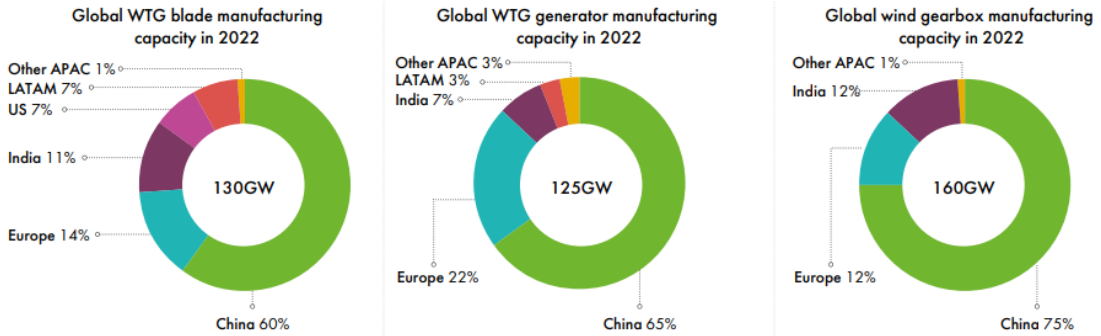

Fig. 2 Production capacity of major wind turbine components
(Left: Blade; Center: Generator; Right: Gearbox) [5]

Wind turbines used for wind power generate on are classified into horizontal-axis wind turbines (HAWT) and vertical-axis wind turbines (VAWT). HAWT are widely used for wind power generation. Figure 3 shows a photograph of a HAWT. Figure 4 shows a photograph of a VAWT.

Fig. 3 Horizontal-Axis Wind Turbine [6]

Fig. 4 Vertical-Axis Wind Turbine [7]

HAWT, which are mainly used in large-scale wind power generation, depend on wind direction for their driving force. Therefore, they are built on beaches or mountain tops where wind conditions are stable, and then the landscape will be greatly changed. Roads for transporting materials to build wind turbines are sometimes constructed by cutting down forests, which have a large environmental impact [8].A wide variety of wild birds inhabit these environments, and there have been several accidents in which birds have died after contacting wind turbine blades during flight [8].For these reasons, residents may oppose the construction of wind turbines.

VAWT, the focus of this study, has the advantage of being omnidirectional, meaning that their drive is independent of the wind direction. Whereas the self-starting capability and power generation efficiency of VAWT are inferior to those of HAWT, and it is assumed that they are not widely used. In this study, the annual average wind velocity in Onahama, Iwaki City, Fukushima Prefecture is used as the target for VAWT's self-starting capability.

VAWT are classified into "lift type" and "drag type" according to the blade shape. The lift type is a wind turbine that uses the lift force generated by the difference in flow velocity between the upper and lower surfaces of the blades to rotate. It has a high peripheral velocity ratio λ(ratio of wind velocity to the peripheral velocity of blade tip of the wind turbine) and excellent torque generation. It means that the wind turbine can generate in higher rotation speed than wind. But lacks self-starting capability. The drag type tends to have excellent self-starting performance, but the peripheral velocity ratio λ cannot exceed 1[10]. It means the wind turbine can't drive faster than the wind velocity. Self-starting performance can be improved by resolving these disadvantages of each blade shape. It will contribute to enhancing the performance of VAWT. Improved performance of VAWT will lead to the introduction of wind power generation in urban areas where wind conditions are unstable. It is expected to reduce the risk of accidents with wild birds. Furthermore, the system is expected to contribute to the further expansion of the share of renewable energy by enabling households and businesses to generate their own power.

2. Previous research

Studies to improve the self-starting performance and power generation efficiency of VAWT have included the use of wind collectors and other devices. Watanabe et al. [11] conducted numerical calculations and wind tunnel

experiment to clarify the flow characteristics around a VAWT. In their experiment, VAWT with a diameter of $D_{wt} = 0.7$ m and two NACA0018 lift-type straight blades are rotated with a peripheral velocity ratio of $\lambda = 2$. They find wind velocity upstream of the turbine is reduced to about 60% and 10% downstream of the wind velocity in relation to the near-by wind velocity. VAWT greatly slows down the wake flow when it is driven. Figure 5 shows a schematic diagram of the experimental setup of Watanabe et al. This wind turbine is equipped with a diffuser and inlet to accelerate the wind upstream of the wind turbine. In an experiment with this wind turbine, the output was increased by a factor of up to 2.6. From this experiment, it was found that the use of a wind intake panel increased the power output.

Figure 6 shows the difference in power output for an experimental wind turbine with different brim sizes. The output is increased by replacing the wind intake panel with a larger brim. However, the wind intake panel is only effective when it is parallel to the wind direction. The non-directionality, which is an advantage of the VAWT is lost if the wind intake panel is fixed.

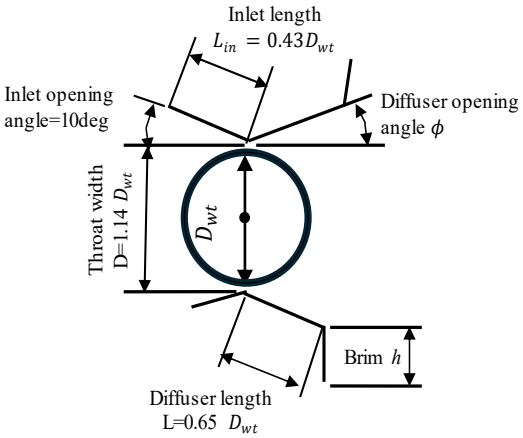

Fig. 5 Drawing of VAWT equipped with wind intake panel [11]

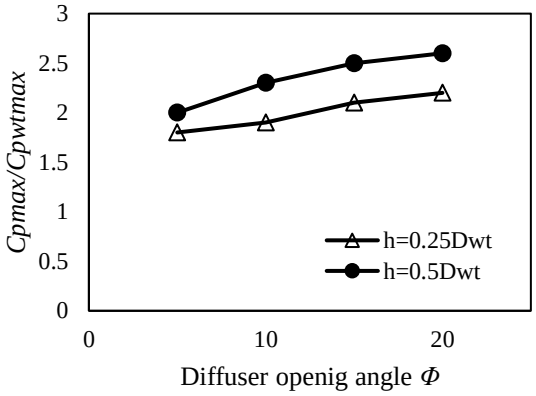

Fig. 6 Change in performance with using wind intake panel [11]

Maruyama et al. investigated the effects of self-starting wind velocity measurements and wind disturbance on a vertical axis wind turbine for use in an urban area [12]. Experiments were conducted in a wind tunnel using a VAWT with three NACA0015 blades of 200 mm rotating diameter, 50 mm blade string length, and 200 mm blade length. Self-starting wind velocity was confirmed at 17.9 m/s in a uniform flow. It starts at 14 m/s when spires and roughness blocks are installed to disturb the flow (power exponent $\alpha = 0.27$). This experiment showed that placing wind turbines near structures can improve self-starting performance. This makes it necessary to carefully select the location of VAWTs.

Thus, no definitive solution has yet been identified to improve the self-starting performance and power output of VAWTs, and research continues to improve blade geometry.

The aim of this study is to improve the self-starting performance of VAWTs while maintaining their non-directional characteristics by improving the blade shape. To achieve this objective, compare the performance of existing blade shapes and prototype blade shapes equipped with blade end plates and flaps through wind tunnel tests and numerical fluid dynamics analysis, and to investigate blade shapes that contribute to improving self-starting performance.

3. Methodology

To estimate the blade shape that improves the self-starting performance of VAWT, this study measures, compares, and evaluates the performance of several types of blade shapes under constant wind conditions, and examines blade shapes that generate high torque at low wind velocity (about 2~5 m/s). As a basis for the performance evaluation, the authors measured the torque of the wind turbine in a wind tunnel and computed a CFD simulation of the blade shape model. Wind tunnel experiments are used to measure power performance under real-world conditions. The advantage of CFD simulation is that the results are not affected by the condition of the experimental setup or disturbances.

3.1. Torque measurement of a wind turbine by wind tunnel experiment

The torque Q and number of rotations n of the rotating wind turbine are measured against wind velocity V. Similar measurements were performed with different blades. The torque coefficient C_q is calculated in Eq. (3.1) that is a dimensionless number to evaluate wind turbine's performance represents the amount of torque that can be generated against the wind velocity and wind-receiving area.

$$C_q = \frac{Q}{0.5\rho A V^3} \tag{3.1}$$

Where, $\rho[\mathrm{kg}\ /\ \mathrm{m}^3]$ is the air density, $A[\mathrm{m}^2]$ is the wind-receiving area, and $V[\mathrm{m}\ /\ \mathrm{s}]$ is the wind velocity.

3.2. CFD simulation using SolidWorks

The coefficients of lift C_L, coefficient of drag C_D, and moment of rotation of the wind turbine at wind velocity of 2 m/s or 5 m/s are computed using SolidWorks Flow Simulation, a computational fluid dynamics (CFD) software. CFD is a computer simulation of the flow around blades, so it is not affected by the conditions of the experimental apparatus and disturbances, and the flow visualization around the blade is easier. The coefficients of lift C_L and coefficient of drag C_D are obtained by equations (3.2) and (3.3), respectively.

$$C_L = \frac{L}{0.5\rho S V^2} \tag{3.2}$$

$$C_D = \frac{D}{0.5\rho A V^2} \tag{3.3}$$

Where, $L[\mathrm{N}]$ is the lift force, $\rho[\mathrm{kg/m}^3]$ is the fluid density, $D[\mathrm{N}]$ is the drag force, $S[\mathrm{m}^2]$ is the reference surface area, and $A[\mathrm{m}^2\ ]$ is the wind-receiving area.

The computational domain and dimensions used to compute C_L and C_D is shown in Fig. 7. Figure 8 shows the computational domain and dimensions used to compute the moment around the z-axis of the wind turbine and 3D simulations. The wind turbine model is not rotated in this study.

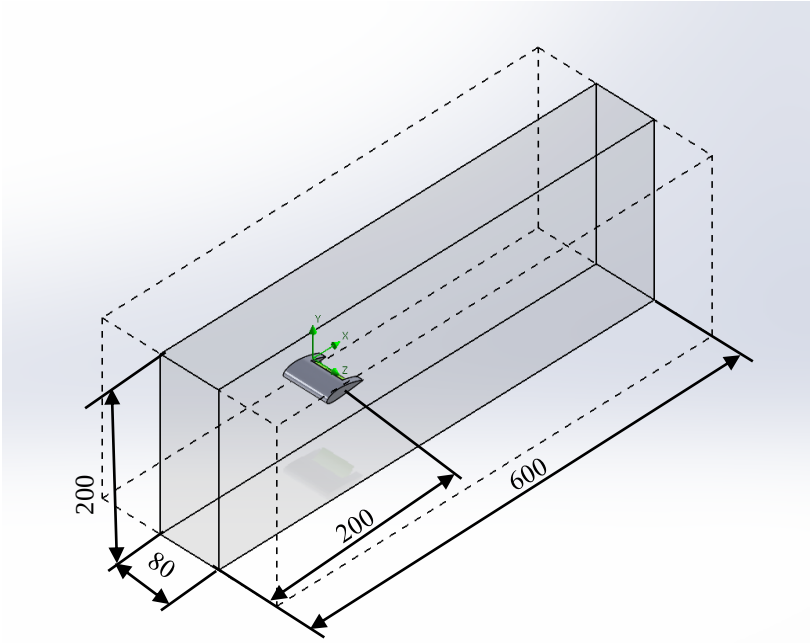

Fig. 7 Computational domain in lift computation

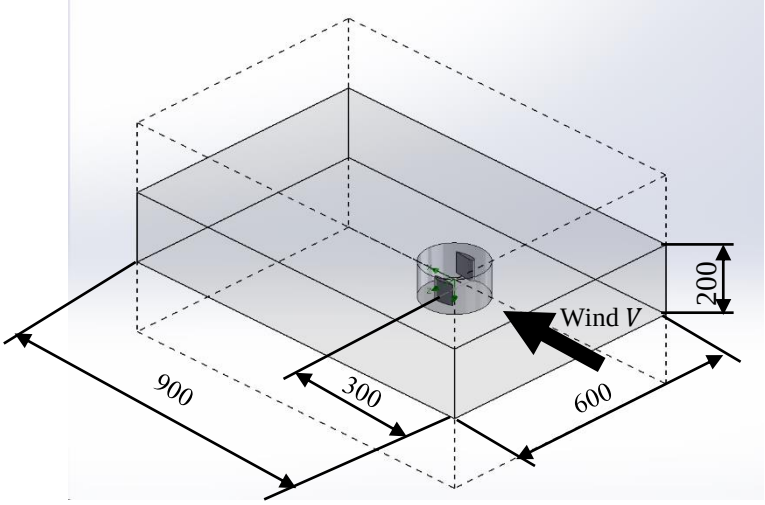

Fig. 8 Computational domain in CFD 2D and 3D moment simulation

Figure 9 shows the mesh setup used in the computation of the lift force derivation for NACA4421. The computational domain mesh in SolidWorks Flow Simulation is based on an orthogonal grid "base mesh" that ignores fine geometry. The mesh around the blade is re-subdivided to improve computational accuracy because flow around the blade is highly variable.

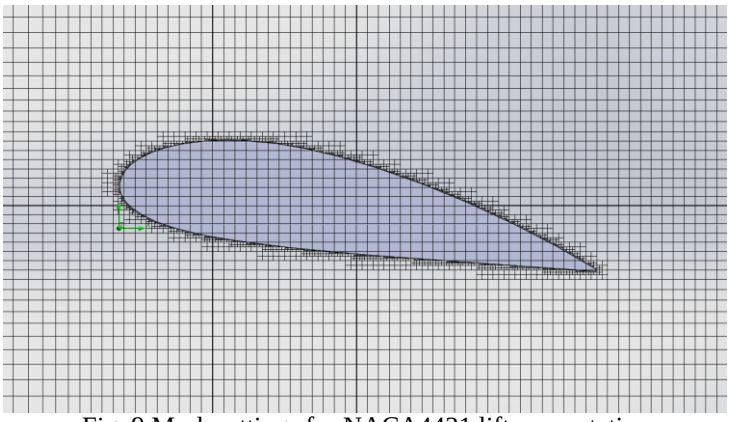

Fig. 9 Mesh settings for NACA4421 lift computation

3.3. Experimental equipment

Figure 10 shows a full view of the wind tunnel apparatus. It is an Eiffel-type wind tunnel with a rectifying section width of 630 ×height of 630, an aperture length of 650, and a measuring section width of 200 × height of 200 × length of 400. A VAWT with a rotating diameter of 100 mm is installed in the measurement section. Experiment is conducted with existing blades and prototype blades.

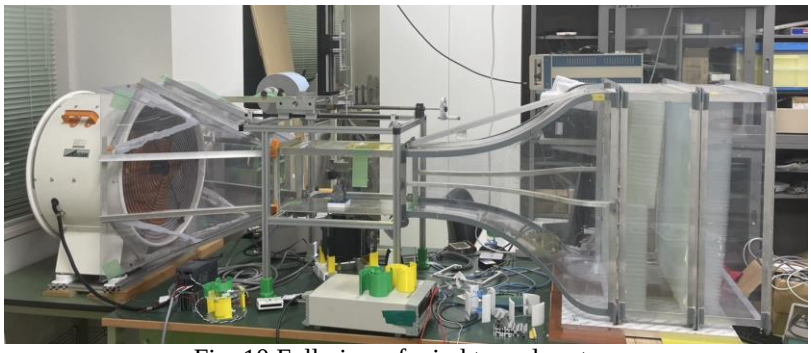

Fig. 10 Full view of wind tunnel system

Figure 11 shows the Savonius wind turbine blade, henceforth referred to as the “Savonius blade”, using in this experiment. It is used as a representative example of an existing drag-type blade to be compared. This blade is considered to have high self-start performance because of its large torque coefficient at low peripheral velocity ratios. Figure 12 shows the detailed dimensions of the Savonius blade, and Fig. 13 shows the dimensions of the wind turbine with the Savonius blade. The blade string length is 60 mm.

Fig. 11 Experimental Savonius blade

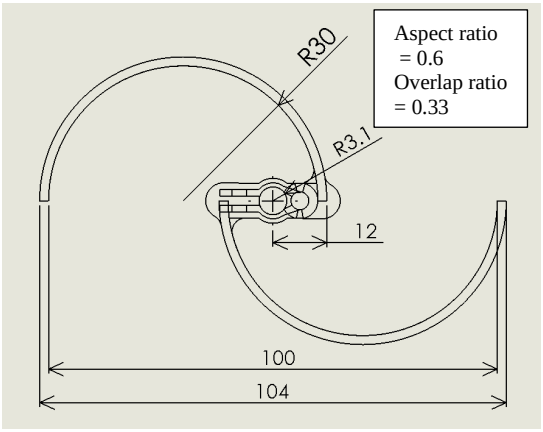

Fig. 12 Savonius blade dimensions

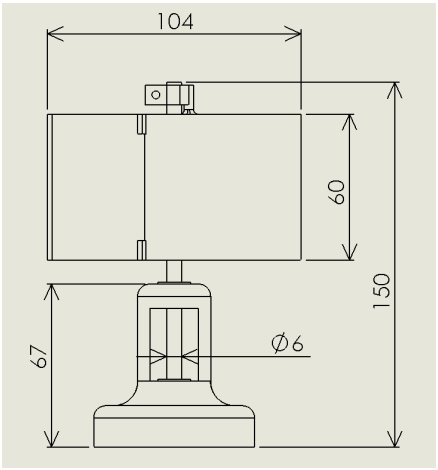

Fig. 13 Dimensions of experimental wind turbine (equipped with Savonius blade)

Fig. 14 Savonius blade with end plates

Figure 15 shows the NACA4421 blade. NACA4421 is an asymmetric blade used as an existing example of a lift-type blade. The asymmetric blade has the characteristic of generating lift by creating a velocity difference between the upper and lower surfaces of the blade even when the blade angle of attack α is 0 degrees.

Four blades were used for comparison with existing blades. Figure 14 shows the Savonius blade with blade end plates. It has 120 mm diameter disks assembled at the top and bottom edges of the Savonius blade. Figure 16 shows the small flap blade. It has a 22 mm movable flap on a portion of NACA 4421 blade. Figure 17 shows the large flap blade. This is a blade with a flap extended to 30 mm in length. Prototype Savonius blade shown in Fig. 18 has two buckets, upper and lower, with a rotational phase difference of 90 degrees. It was made to investigate the effect of the number of Savonius buckets on self-starting performance.

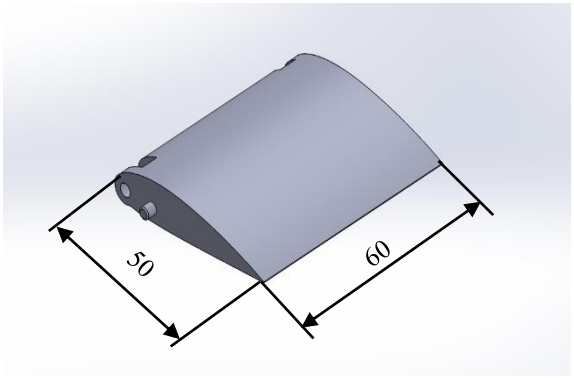

Fig. 15 NACA4421 blade

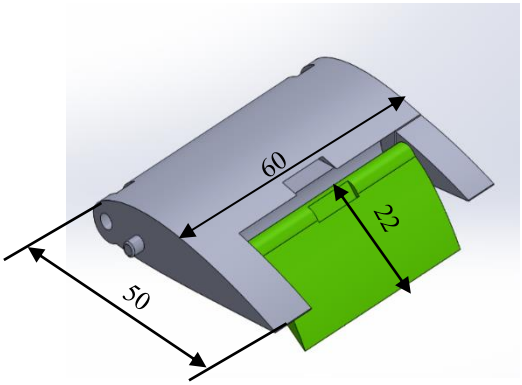

Fig. 16 Small flap blade

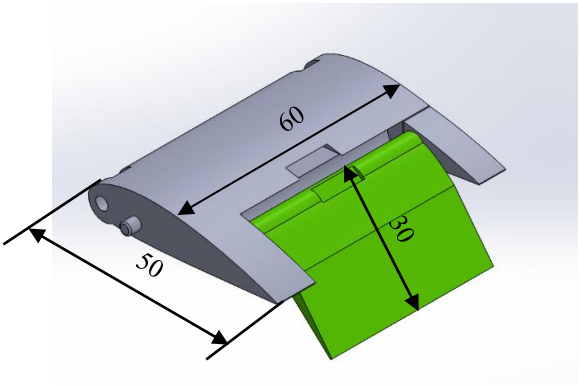

Fig. 17 Large flap blade

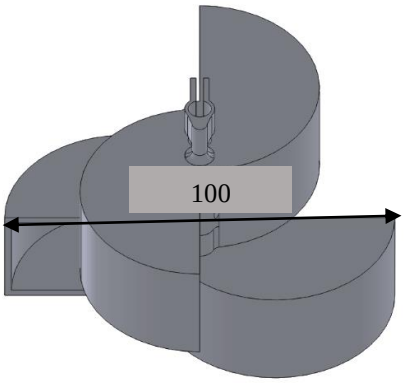

Fig. 18 Prototype Savonius blade

Figure 19 shows the configuration of the measurement device. A torque meter SS-005 is connected to the rotating shaft of the wind turbine through a coupling and a generator is connected to the driven side. The generator generates 7 V at 1000 rpm and has an internal resistance of 150 Ω. The generator is connected to a 930 Ω resistor and an LED. A rotation detector MP-981 is mounted on the torque meter to simultaneously measure the number of rotations of the wind turbine. Table 1 shows the specifications of the torque meter.

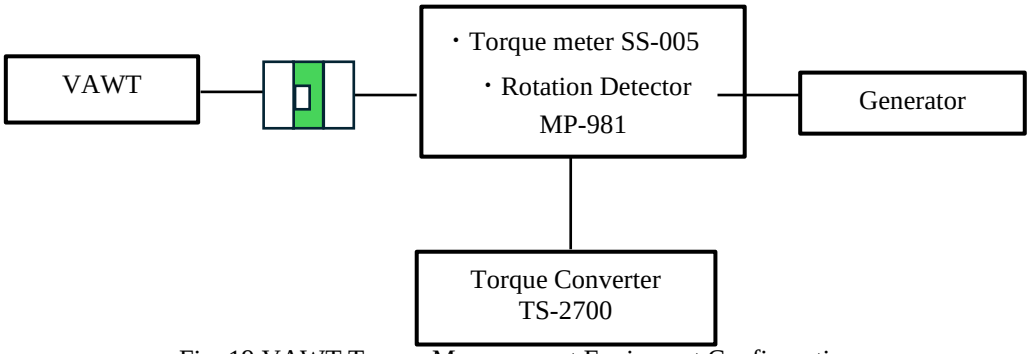

Fig. 19 VAWT Torque Measurement Equipment Configuration

Table 1 Specifications of Torque meter SS-005

Torque rate [N-m]	0.5
Moment of inertia[kg・cm^2]	0.425
Spring constant[N-m/rad]	41.2
Number of gear teeth for rotation detection	60
Maximum rotation [rpm]	6000
Power consumption[W]	35
Measurement Accuracy [%]	±0.2FS

The blower, Suiden SJF-T506, is connected to a PC via an inverter, Mitsubishi Electric FREQUAL-E700.

The wind velocity measured by the pitot tube is used as the wind velocity in the wind tunnel. Pitot tube consists of a static pressure tube and a total pressure tube, and the wind velocity is obtained from the differential pressure between them. Equation (3.4) shows the formula for deriving wind velocity using a pitot tube.

$$V = \sqrt{\frac{2(p_0 - p)}{\rho}} \tag{3.4}$$

Where, p_0[Pa] is the pressure measured by the total pressure tube, p[Pa] is the pressure measured by the static pressure tube, and ρ[kg / m^3] is the density of air.

4. Findings

4.1. Wind velocity measurement results

Figure 20 shows the results of flow velocity measurements using a pitot tube. The maximum flow velocity in the wind tunnel is about 13 m/s. The average measurement error is about 6% when compared to the ring vortex anemometer [(13)], which determines the flow velocity from the Karman vortex shedding frequency. The error was 9.2% at a wind velocity of 2.0 m/s, the error was 3.7% at a wind velocity of 10 m/s. From these results, Measurements by pitot tube at low wind velocity (wind velocity up to 2.0 m/s) are not reliable because the differential pressure is small.

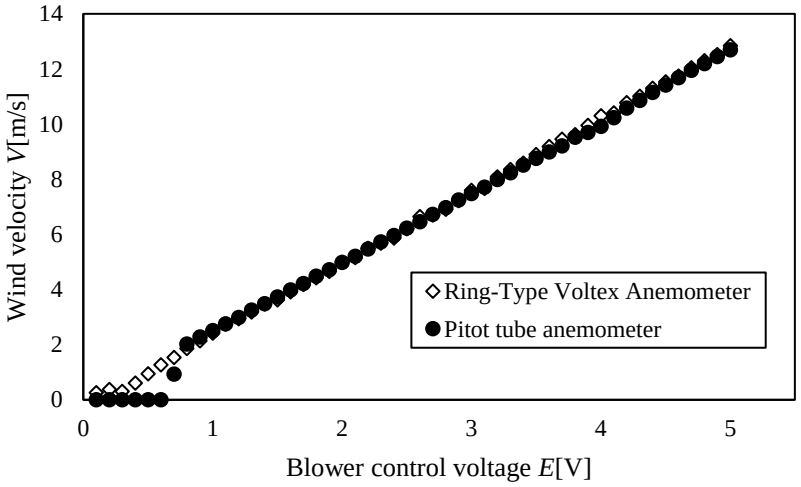

Fig. 20 Wind velocity relative to blower control voltage

4.2. Torque measurement results and self-starting property evaluation of Savonius blade

Table 2 shows the self-starting wind velocity for the tested blades. None of the blade shapes used in this study self-started at a wind velocity of 2.0 m/s. The minimum self-starting wind velocity before installing the torque meter was 4.2 m/s, but after the torque meter was installed, it was 10.4 m/s. It is thought that the torque meter increases the resistance, such as static friction force etc., on the wind turbine's rotating shaft, making it more difficult for the turbine to rotate. The maximum wind velocity in the wind tunnel was about 13 m/s, which narrowed the range in which the rotational torque could be measured.

Table 2 Self-starting wind velocity for each blade shape [m/s]

Savonius blade	12.6
NACA4421(2 blades)	No startup
NACA4421(3 blades)	No startup
NACA4421(4 blades)	No startup
Prototype Savonius blade	10.2
Small flap blade	No startup
Large flap blade	No startup
Savonius blade with end plates	No startup
PET Savonius blade	No startup

Figure 21 shows the torque evolution of the Savonius blade against wind velocity. In the Savonius wind turbine, the torque continues to increase from a wind velocity of about 2.0 m/s and reached its maximum value at a wind velocity of about 8.0 m/s, and signs of rotation like slight shaking of the blades were observed. But the turbine stopped shortly after. Figure 22 shows the blade attitude when the torque is decreasing at the wind velocity of 8.0 m/s in Fig. 21. Drag and rotational force are generated when the bucket faces directly upwind based on the rotation principle of drag-type wind turbines including Savonius blades. It is considered that rotational torque decreased because concave part of the bucket is not exposed to the wind in Fig. 22.

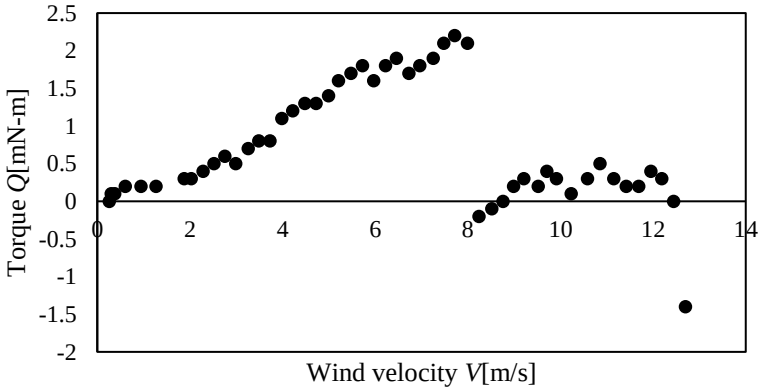

Fig. 21 Wind velocity and torque transition of Savonius blade

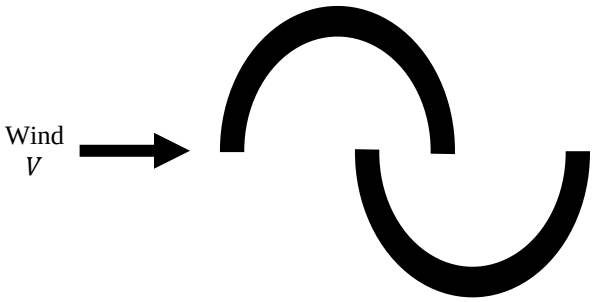

Fig 22 Attitude of the blade has rotation stops

Based on these results, the authors considered that the existing single-stage bucket Savonius blade would be disadvantageous for self-starting depending on the rest attitude, so produced a two-stage bucket Prototype Savonius blade, shown in Fig. 18 and conducted similar experiment. The two-stage bucket Prototype Savonius blade self-started at a wind velocity of 10.2 m/s, having one bucket facing directly upwind allows for self-starting regardless of the rest position of the wind turbine.

4.3. Variation of the torque generated by the Savonius blade at different blade attitudes computed by CFD

As shown in Table 2, most of the blades either did not self-start in the wind tunnel tests or started in winds stronger than the target. Therefore, the results are not useful for evaluating the performance of wind turbines at low wind velocities. The authors decided that CFD is more effective than wind tunnel experiments for visualizing the forces generated by the blades and the flow at low wind velocities, so calculations were performed.

First, the reduction in torque due to blade attitude observed in wind tunnel experiment was simulated using CFD. Figure 23 shows the posture of the blade model during the computation. The difference in rotational moment generated by the left (bucket not facing the wind) and right (bucket facing the wind) is compared. The rotating diameter is 100 mm, the blade thickness is 2 mm, and the wind velocity is 2.0 m/s in the x direction, with no rotation.

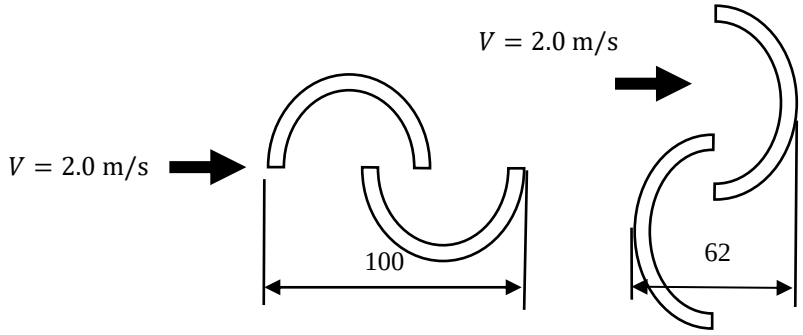

Fig. 23 Attitude of Savonius blade during CFD simulation
(Left: not facing the wind; Right: Facing the wind)

In Fig. 23, Reynolds number $Re = 13503$ for the left blade attitude and $Re = 8208$ for the right blade attitude. Reynolds numbers above 2300 are considered turbulent. Since the conditions of these computations can be considered turbulent, a k-ε turbulence model was introduced into the analysis setup. The number of computed cells was 32416, of which 14772 were tangential to the blade. The computation results are shown in Table 3. As in the wind tunnel experiment, the bucket generates a large torque when it is facing directly into the wind. From these results, Savonius blade needs the blade shape, and some ingenuities should be such that the concave part of the bucket is facing directly upwind.

Table 3 Difference in rotational moment due to Savonius blade attitude ($V = 2$ m/s)

	Not facing the wind	Facing the wind
Moment of Z axis [mN · m]	0.98326	2.64977
Drag force[mN · m]	39.3305	105.991

The magnitude of the CFD-computed rotational moment is larger than the torque measurement results shown on Fig. 21. The blade tip effects are minimized because the computation is performed in a 2D domain. And only simple blade without detailed parts were simulated. The amount of torque generated in wind tunnel experiment is affected by friction and other factors applied to the rotating shaft. The authors assume that these are the reasons for the difference between the wind tunnel experiment results and the CFD analysis results. However, the tendency for the torque to increase when the blade is directly upwind is consistent. In the future, CFD computations of the entire wind turbine model, not just the blades, will help reproduce actual conditions of use and facilitate comparison of results with wind tunnel experiments.

4.4. Verification of the blade tip plate effect of the Savonius blade

The performance of Savonius blades with and without end plates (see Fig. 14) are compared based on wind tunnel tests and CFD results. Figure 24 compares the torque generated by the Savonius blades with end plates or non-end plates. Figure 25 compares the torque coefficient C_q corresponding to the torques in Fig. 24. In these experiment results, both torque and torque coefficient for Savonius blade with end plates are higher than those of non-end plates at wind velocity of 3~5.5 m/s. The maximum difference is 1.0 mN·m in torque and 53% in C_q at a wind velocity of 5.5 m/s.

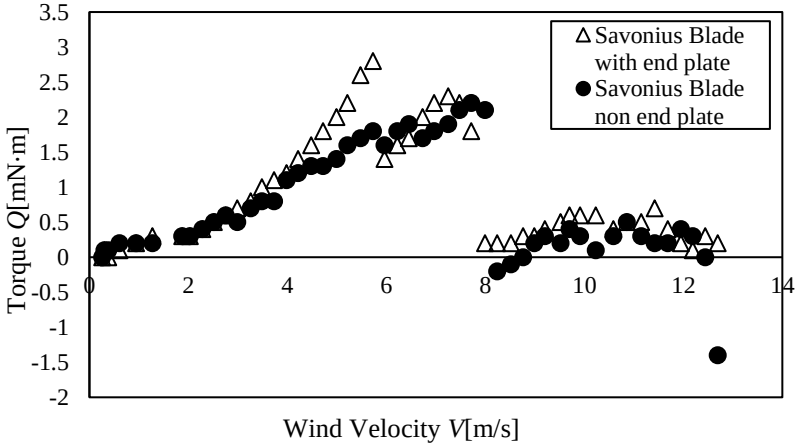

Fig. 24 Comparison of torque generated with and without blade end plates

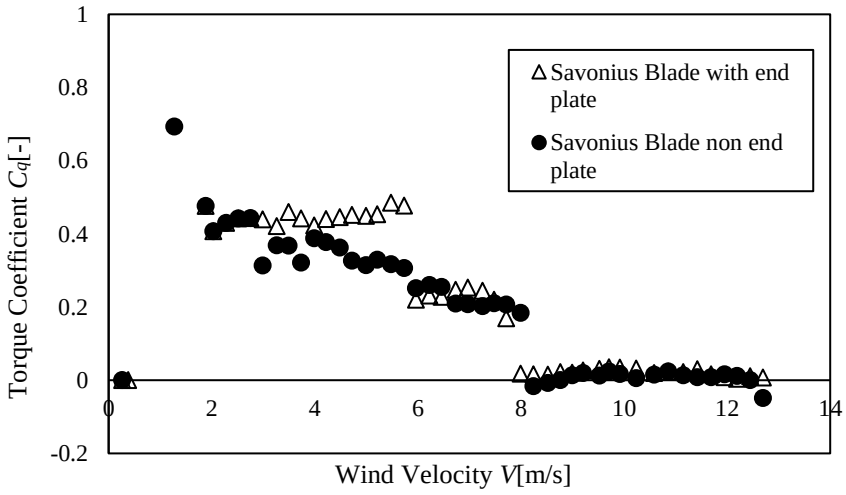

Fig 25 Comparison of torque coefficients with and without end plates

Figure 26 and Fig. 27 show the flow around a Savonius blade with and without end plates, respectively. The use of end plates suppresses wind outflow in the vertical direction of the blades. Whereas the flow velocity near the blade is reduced upstream of the blade.

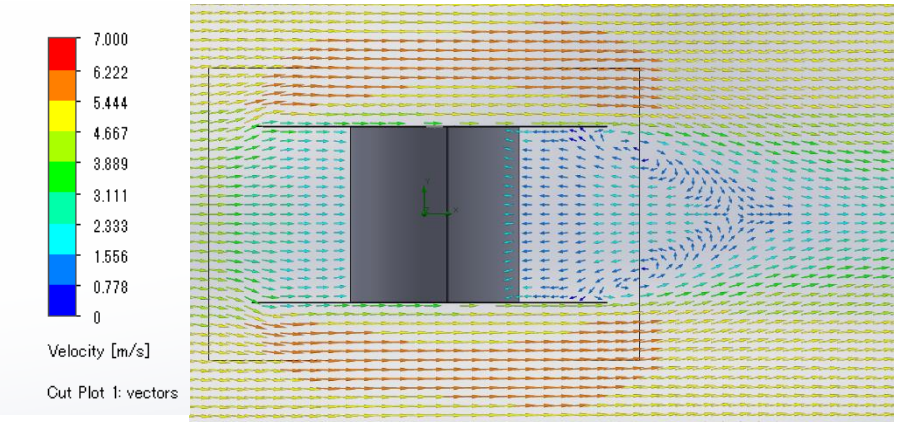

Fig 26 Side view of wind velocity vectors around a Savonius blade (with end plates) (V=5 m/s)

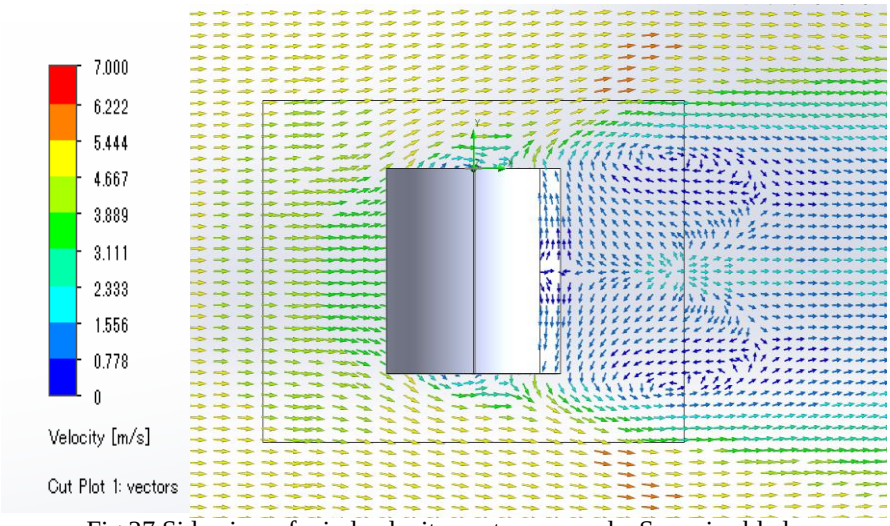

Fig 27 Side view of wind velocity vectors around a Savonius blade (non-end plates) (V=5 m/s)

4.5. Wind tunnel test results and CFD simulation results of the lift-type wind turbine

The lift-type blades (NACA4421, Small flap blade, and Large flap blade) did not self-start in the wind tunnel experiment. The maximum torque generated was 0.7 mN·m, which was 1/7 that of the Savonius wind turbine. The weight of the rotating part of the three blades is 125.1 g, which is about four times that of a Savonius blade. In previous research by Maruyama et al. [(12)], a lift-type wind turbine with a rotating diameter of 200 mm required a self-starting wind velocity of 17.9 m/s. Self-starting is difficult at experimental wind velocity of 13 m/s or less in this study.

Table 4 Number of calculation cells for each blade

	Total number of cells	Cells tangential to blade	*Re*
NACA4421	79584	35174	16548
Small flap blade	86436	39596	15389
Large flap blade	60974	28594	17100

The effectiveness of the flaps could not be evaluated from the wind tunnel experiment since the wind turbine did not start. Therefore, the lift force and the flow around the lift-type blades were obtained from CFD simulations and compared. The number of computed cells for each blade shape is shown in Table 4. Figure 28 through 31 show the flow when wind velocity is 5 m/s around the NACA4421 blade at angles of attack of 0° and 10°, the small and large flap blade. The flap deployment angle is 30 degrees relative to the blade string line of the NACA4421 blade.

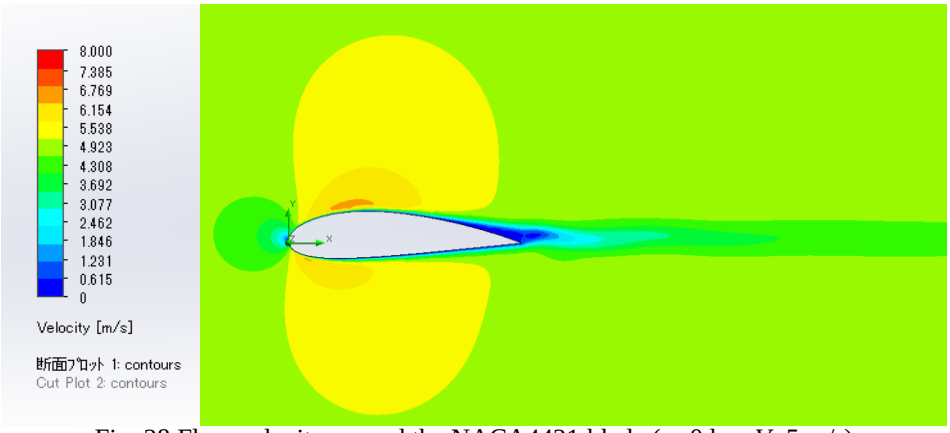

Fig. 28 Flow velocity around the NACA4421 blade (α=0deg, V=5 m/s)

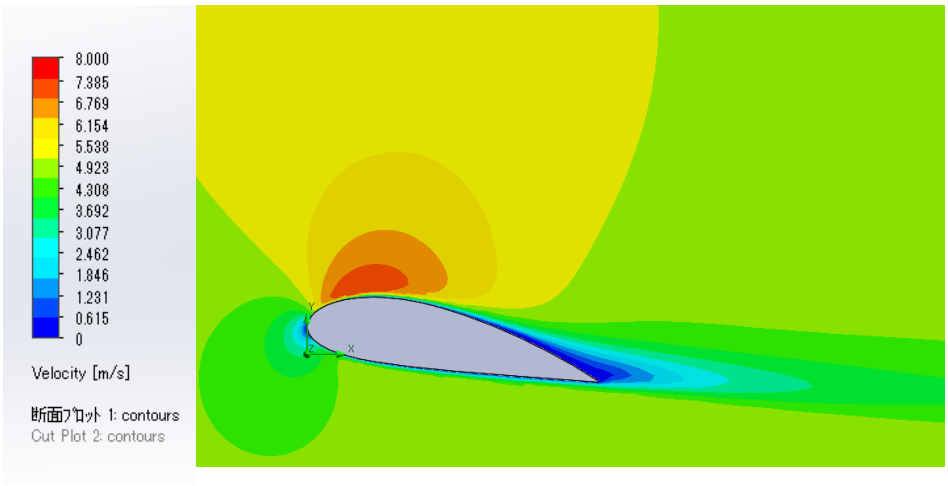

Fig. 29 Flow velocity around the NACA4421 blade (α=10deg, V=5 m/s)

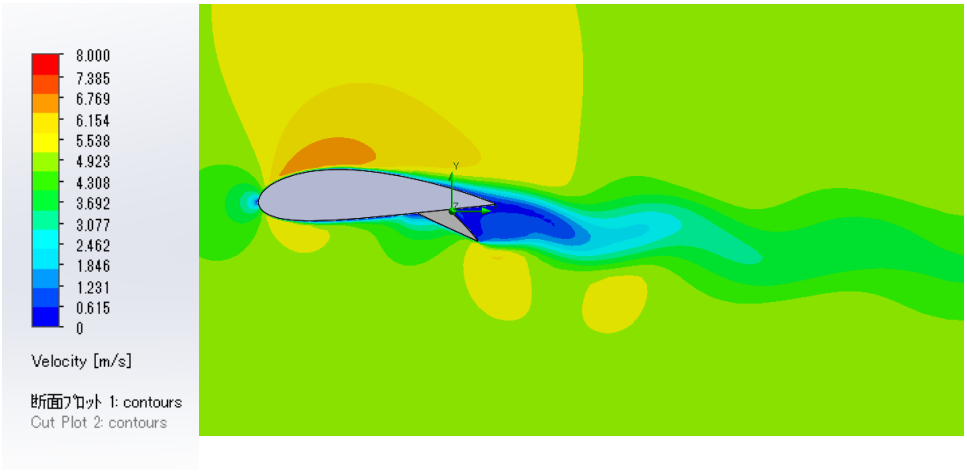

Fig. 30 Flow velocity around the small flap blade (V=5 m/s)

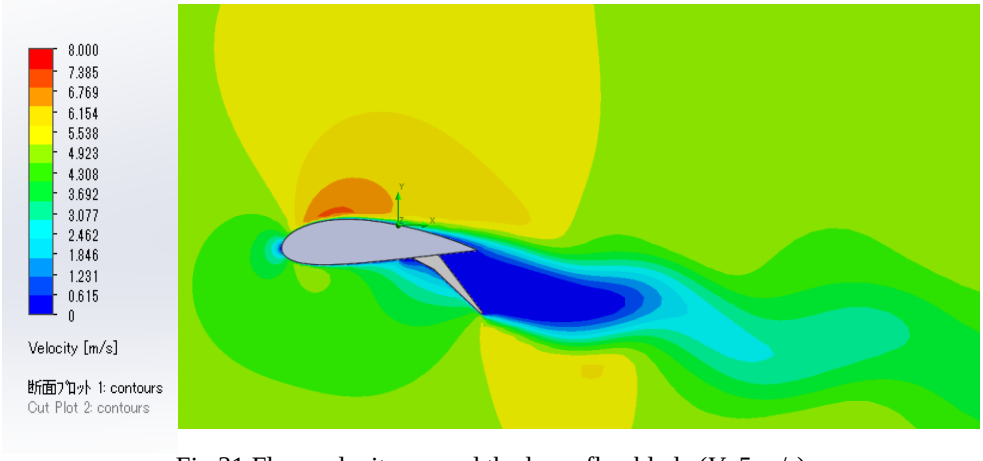

Fig 31 Flow velocity around the large flap blade (V=5 m/s)

Compared to the NACA4421 blade, the flap-mounted blade has a further decrease in flow velocity of about 2 m/s in the flap wake. The flap reduces the flow velocity, which is thought to create drag. Flow velocity on the underside of the large flap blade is about 1.5 m/s lower than that of the small flap blade. Therefore, the authors inferred that flap deployment contributes to the increase in drag. Table 5 shows the computed drag force D, lift force L, drag coefficient C_D, and lift coefficient C_L for the above four types of blades. Both lift and drag increase when the flaps deploy. Flap leads to increase in the lift force because the flaps slow the flow velocity on the lower surface of the blade. It can be inferred that the installation of flaps on lift-type wind turbine blades contributes to the improvement of self-starting performance due to the increased lift. Flap deployment to prevent over-rotation during operation at high peripheral velocity ratios is also considered to be useful since the flaps also increase drag.

Table 5 Comparison of lift and drag of lift-type airfoils

	D[mN・m]	L[mN・m]	C_D	C_L
NACA4421(α = 0deg)	5.25	1.85	0.54	0.04
NACA4421(α = 10deg)	11.70	63.43	0.96	1.42
Small flap blade	19.21	44.63	1.45	1.08
Large flap blade	30.52	75.75	1.86	1.87

The shortcomings of VAWTs are eliminated by achieving improved self-starting performance and maintaining power generation capability at high peripheral speed ratios. The improved performance of VAWTs enables them to generate power not only in mountainous areas but also in urban areas by taking advantage of their omni-directional nature. Currently, photovoltaic power generation is the main method of home power generation. The same could be done with VAWT. These factors are expected to increase the use of renewable energies and further promote home power generation. Reducing dependence on major electric power companies, which generate a large proportion of their electricity from thermal power, is expected to indirectly contribute to reducing CO2 emissions.

But there is concern that the number of parts may increase due to the use of flaps, resulting in higher costs. In addition, there is a risk of noise and damage during flap operation. In the future, it will be necessary to design blades with the aim of safely implementing the flap mechanism and reducing costs by simplifying the mechanism. The authors are designing a morphing blade in which the entire blade is elastic and elastic. This is expected to reduce the number of parts while maintaining the flap function.

5. Conclusions

In this study, to improve the self-starting performance of vertical axis wind turbines, the authors worked on clarifying the dynamic characteristics of existing blade shapes and investigated and produced blade shapes that contribute to self-starting performance. Two existing wind turbine blades, NACA4421 and single-stage Savonius blades, and four prototype blades, including Savonius blades with end plates and lift-type flap blades, were built. Then, the torque generated by the wind turbine was measured in the wind tunnel and the lift and drag forces were computed by CFD simulations. The results were obtained as follows.

I. The minimum self-starting wind velocity was 10.2 m/s.
II. For Savonius blades, if the bucket recess does not face upwind, the torque decreases, and the wind turbine stops.
III. Torque increased by up to 55% when the blade was equipped with blade end plates at the top and bottom edges. The end plates prevent wind from flowing out of the top and bottom of the blade.
IV. When the lift-type blade is equipped with flaps, the lift and drag forces increase due to the reduction of the flow velocity on the underside of the blade.

It was not possible to create a wind turbine blade that could self-start at the target wind velocity of 2.0 m/s. For lift-type wind turbines, it is expected that the self-starting performance can be improved by increasing the lift by installing flaps. For Savonius wind turbines, self-starting performance could be improved by increasing the number of buckets or by attaching blade end plates.

.

Acknowledgments

I am grateful to students in the author's laboratory, for their help in improving the wind tunnel apparatus and in using SolidWorks Flow Simulation. I would like to express my deepest gratitude to him.

References

(1) Japan meteorological Agency website. Secular Change in Global Annual Mean Temperature Anomalies (1891-2023: Preliminary Figures). (in Japanese).Date viewed: December 6, 2024.https://www.data.jma.go.jp/cpdinfo/temp/an_wld.html
(2) Agency for Natural Resources and Energy website. Japan's Energy 2022: 10 Questions to Know About Energy Today. (in Japanese).Date viewed: December 6, 2024.https://www.enecho.meti.go.jp/about/pamphlet/energy2022/007/
(3) Japan Wind Power Association. Wind Power Generation in Japan (as of the end of June 2022). Date viewed: December 8, 2024 https://jwpa.jp/information/6655/
(4) GWEC. GLOBAL WIND REPORT 2023. pp.8, pp.52 .Date viewed: January 25,2025 .https://gwec.net/wp-content/uploads/2023/04/GWEC-2023-interactive.pdf
(5) GWEC. above. pp.27
(6) Maeda Corporation website. Happo Wind Power Generation Project. Date viewed: December 25, 2024 (in Japanese) https://www.maeda.co.jp/works/datsuukeoi/happou/
(7) Nikkei XTECH. (November 24, 2006). Vertical axis type small wind power generation that works in light wind. (in Japanese) .Date viewed: December 6, 2024.https://xtech.nikkei.com/kn/article/building/info/20061120/501156/
(8) Yuko Hayashi & Saiko Shiraki & Osamu Hasegawa. (2012). Considering the impact of wind power on ecosystems. *Japanese Journal of Conservation Ecology*, vol.17, pp.81~pp.84 (in Japanese). https://doi.org/10.18960/hozen.17.1_81
(9) Japan-meteorological Agency. Monthly average of Onahama (Fukushima Prefecture) mean wind velocity (m/s). https://www.data.jma.go.jp/obd/stats/etrn/View/monthly_s3.php?prec_no=36&block_no=47598&year=&month=&day=&View=a4
(10) Fumio Matsumoto & Izumi Ushizawa & Yoshifumi Nishizawa. (2011). Vertical Shaft Windmill Manufacturing Guidebook. Power Company. pp. 12 (in Japanese)
(11) Koichi Watanabe & Yuji Ohya & Takashi Karasutani. (2010). Elucidation of Driving Principle of Vertical Shaft Type Wind Turbine and Application of Wind Gathering Devices for Higher Output. *Proceedings of the 21st Symposium on Wind Engineering*, (in Japanese) https://doi.org/10.14887/kazekosymp.21.0.239.0
(12) Yusuke Maruyama & Masayuki Shimura & Ryuichiro Yoshie & Kazuichi Seki. (2000). Development of a Vertical Shaft Type Wind Power Generator with Straight Blades to be Integrated into Buildings. *Proceedings of the 22nd Symposium on Wind Energy Application*. pp. 162 (in Japanese)
(13) Mizuyasu Koide & Tsutomu Takahashi & Masataka Shirakashi. (2001). Trial Manufacture of Ring Anemometer for Measuring Low Velocity in Wind Tunnel Experiments. *Transactions of the Japan Society of Mechanical Engineers*. Vol. 67. No. 657. pp. 3 – 9 (in Japanese). https://doi.org/10.1299/kikaib.67.1105

Authors' Biographies

Yuta ODANAGA is a student at National Institute of Technology, Fukushima College since 2018. My study focuses on mechanical engineering and wind turbines. A thesis for the acquisition of a bachelor's degree has been submitted to the National Institution for Academic Degrees and Quality Enhancement of Higher Education and is currently under review.

Mizuyasu KOIDE received his Ph.D. in engineering from the Nagaoka University of Technology in 2002. I was appointed as lecturer at the Niigata Sangyo University in 2003, and then joined National Institute of Technology, Fukushima College in 2013. In 2022, I became a professor. My research areas are vortex induced vibration, vibration power generation, and wind turbines in fluid engineering. I am also engaged in engineering education activities for elementary and junior high school students, focusing on manufacturing.